Dataset overview.

Layered earth inversion and related airborne geophysical datasets derived from the TEMPEST AEM Survey, Billabong Creek, southern New South Wales, 2001

1.0 Overview

This product contains three airborne geophysical datasets:

- the final geophysical inversion of the Billabong Creek TEMPEST airborne electromagnetic (AEM) survey data using a layered earth inversion algorithm developed by Geoscience Australia (GA-LEI);
- an airborne magnetic, gamma-ray and elevation (MAGSPEC) survey; and
- an extract of the Australian National Gravity Database (GRAVITY).

These data include enhancements of previously available datasets, using more recent geophysical processing software advances.

The airborne geophysical surveys were carried out in the Billabong Creek area, near Albury in southern New South Wales (figure 1 and figure 2).

The Billabong Creek airborne geophysics survey was commissioned by the Murray–Darling Basin Commission in 2001. Fugro Airborne Surveys Pty Ltd (Fugro) was contracted to acquire and process the AEM survey utilising the TEMPEST time domain airborne electromagnetic system. Kevron Geophysics Pty Ltd (Kevron) was contracted to acquire and process the MAGSPEC survey utilising an industry standard system. Both surveys were contracted and project managed by the Australian Government Department of Agriculture, Fisheries and Forestry through the Australian Bureau of Agricultural and Resource Economics and Sciences (formerly Bureau of Rural Sciences), while Geoscience Australia managed and quality controlled the work of Kevron and Fugro.

Additional processing and enhancements of the airborne geophysics data was undertaken by Geoscience Australia in 2007–08, using more recent geophysical processing software advances, with funding from the National Action Plan for Salinity and Water Quality. The AEM reprocessing using the GA-LEI algorithm significantly improved previous conductivity predictions. The Billabong Creek airborne magnetic, gamma ray and elevation surveys were also processed into a range of derivative products specially designed to enable extraction of geologically meaningful information to support salinity and natural resource management.

Figure 3 below gives a graphical overview of the directory structure of this data product.

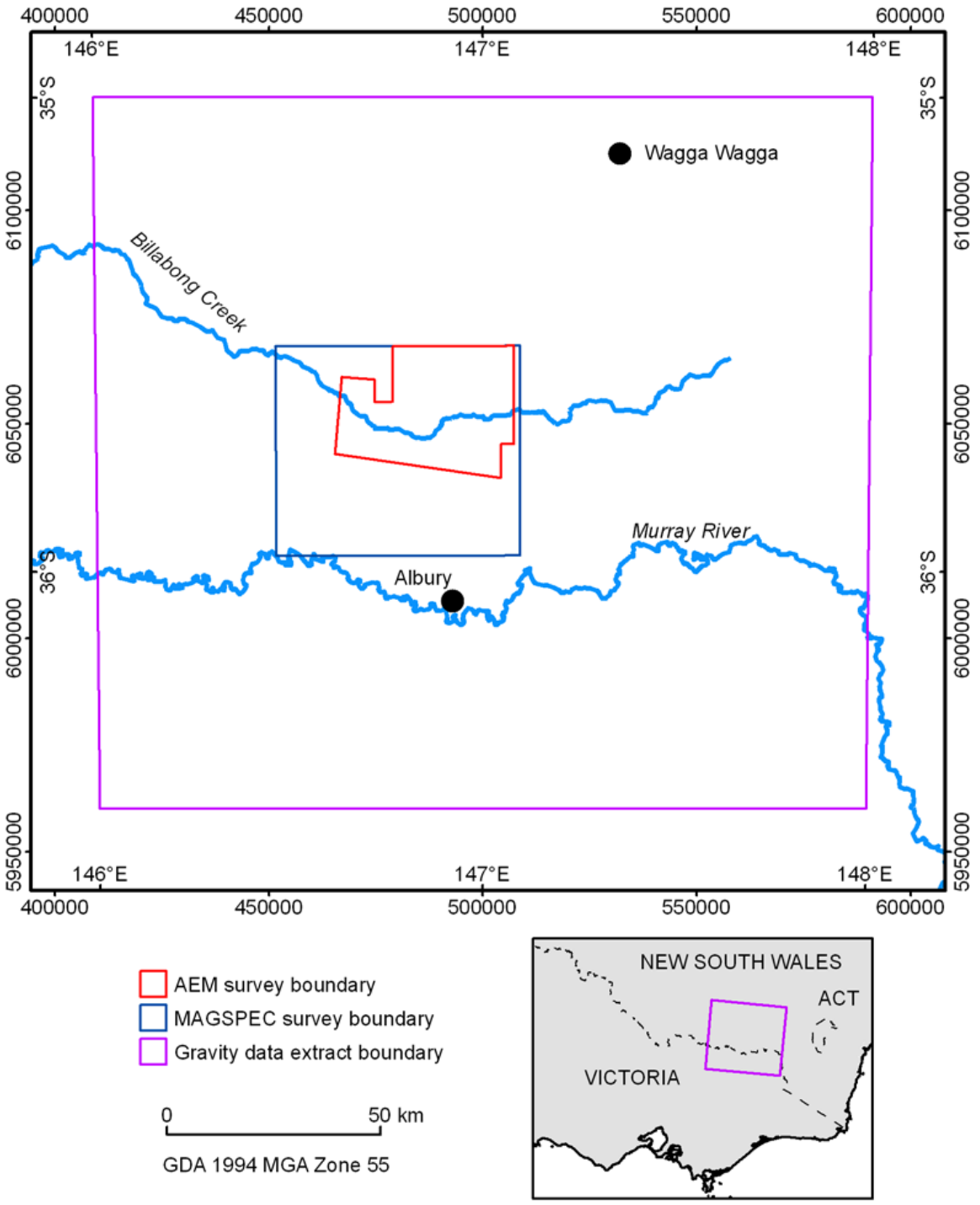

Figure 1 - Location of the AEM and MAGSPEC surveys, and the gravity data extract. Source: Geoscience Australia.

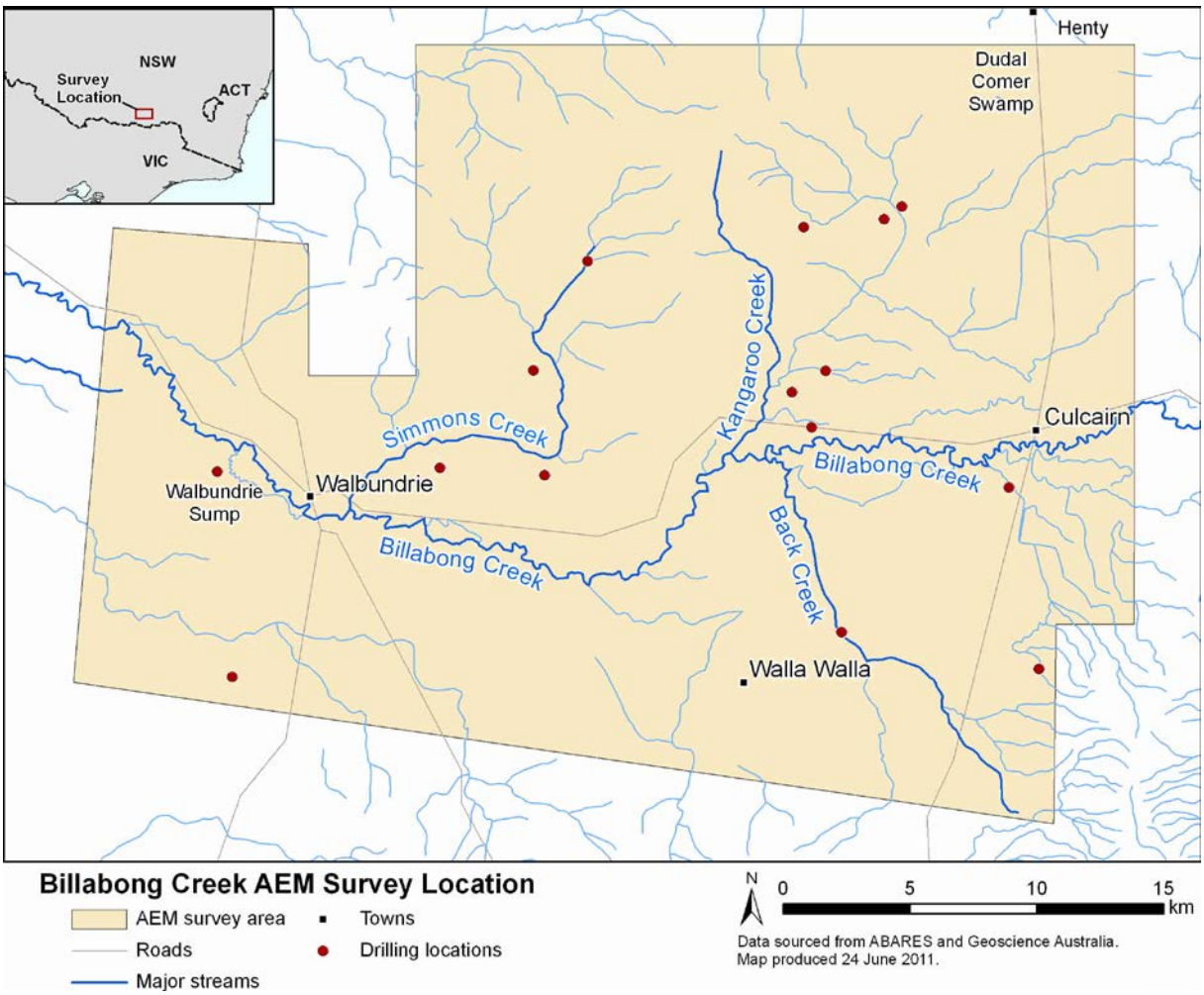

Figure 2 - Location of the Billabong Creek AEM survey area

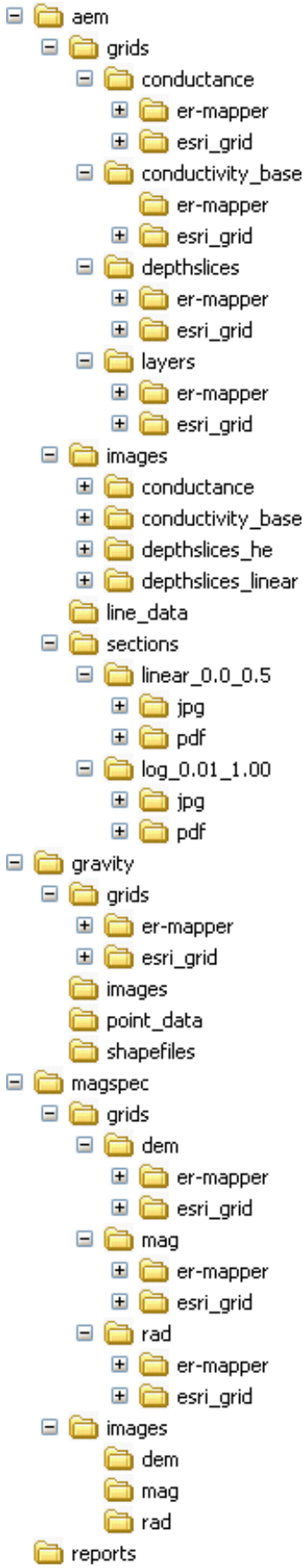

Figure 3: Graphical overview of the directory structure of this data product

The following sections describe the key datasets in this data product.

Appendix 1 gives a detailed list of the contents of each directory and the dataset components.

2.0 Reports (sub-folder: reports).

This data product includes the following reports:

Filename BBC_survey_and_metadata_final.pdf

Description This report describes the processing of the TEMPEST AEM data GA-LEI inversion, MAGSPEC, elevation and gravity data including point located data, grids and derived images which was undertaken by Geoscience Australia.

This report is the key document for this data product.

The first section of the report describes different datasets that have been acquired and processed (processed data), and the second section lists the different products that have been derived from those datasets (derivative data).

Reference Fisher, A. and Brodie, R.C., 2008. Geophysical survey data and metadata, Billabong Creek, New South Wales. Report produced by Geoscience Australia for the Bureau of Rural Sciences, Canberra, Australia.

Filename BBC_Inversion_Report_final.pdf

Description This report describes the processing of the TEMPEST AEM conductivity predictions using the GA-LEI algorithm was undertaken by Geoscience Australia.

This report is the key document for details of the GA-LEI inversion.

Reference Brodie, R.C. and Fisher, A., 2008. Inversion of TEMPEST AEM survey data Billabong Creek, southern NSW. Report produced by Geoscience Australia for the Bureau of Rural Sciences, Canberra, Australia.

Filename BBC_Fugro_AEM_jobreport.pdf

Description This report describes the acquisition and initial processing of the AEM survey data by the airborne geophysical survey contractors Fugro Airborne Surveys.

Reference Owers, M.,Sattel, D. and Stenning, L., 2001. Billabong Creek NSW TEMPEST Geophysical Survey acquisition and processing report. Fugro Airborne Surveys report to the Bureau of Rural Sciences.

Filename HSK_KEVRON_Operations_Processing_Report.pdf

Description The Honeysuckle Creek and Billabong Creek Operations and Processing report was compiled by Kevron Geophysics.

Reference Kevron Geophysics, 2001. Operations and processing report, Honeysuckle Creek and Billabong Creek geophysical surveys. Kevron Geophysics report to the Bureau of Rural Sciences.

3.0 AEM data (sub-folder: aem).

The AEM survey data includes the final geophysical inversion of the Billabong Creek TEMPEST AEM survey data using a layered earth inversion algorithm developed by Geoscience Australia (GA-LEI). The GA-LEI AEM data is derived from the 'Billabong Creek TEMPEST AEM Survey, NSW, 2001 Final Located Data (P904)', available as Geoscience Australia product 65385 (GeoCat #65385). The GA-LEI algorithm has been demonstrated to generate more accurate conductivity predictions than the previous conductivity predictions available in GeoCat #65385 for other similar TEMPEST surveys.

The AEM datasets are:

- line (point located) data of layer conductivity, depths below ground level, and thicknesses. These are the primary data output of the GA-LEI inversion process (sub-folder: aem\line_data)
- grids of the conductivity model layers interpolated from the inversion line data; the layers are relative to ground surface (sub-folder: aem\grids\layers)
- grids of conductivity depth slices of regular thicknesses generated from the layers; the depth slices are relative to natural surface (sub-folder: aem\grids\depth_slices)
- vertical conductivity–depth sections along flight lines (sub-folder: aem\sections); these are graphical representations of the estimated conductivity in a vertical slice along the line of best fit passing through the flight line. These sections were produced for each flight line in the AEM survey (sub-folder: aem\sections).
- a grid and images of conductance distribution produced from the GA LEI results. Conductance is conductivity multiplied by thickness, and is measured in siemens (S) (sub-folder: aem\grids\conductance).
- grids and images of the depth of the base of the conductive unit, using an automated technique applied to the point located GA LEI data (sub-folder: aem\grids\conductivity_base).
- a range of images of the above grid datasets were produced using standard image enhancement techniques (sub-folder: aem\images).

3.1 Line data (sub-folder: aem\line_data)

The results of the GA LEI are stored in a point located (or line) format, in an ASCII file formatted with space-delimited columns. Each record represents one sample along a flight line, which records the conductivity values for the modelled layers. A comprehensive header file is associated with the file, which describes the data and the numeric format of each column in the file.

File name	File description
billabong_creek_tempest.dat	final point located data from the AEM survey (see .hdr file for details)
billabong_creek_inversion.dat	final point located AEM data produced by the GA-LEI (see .hdr file for details)

3.2 Layer conductivity grids (sub-folder: aem\grids\layers)

The layer conductivity grids represent the conductivity in siemens per metre (S/m) of each layer of the 25 layer conductivity model. The data were gridded to a square 40 m cell size from the micro-levelled point located data using minimum curvature gridding . There are always 25 layers in the model and the thickness of each layer is constant over the whole survey area. The layer thicknesses and depth extents are shown in Table 1. All depths are relative to the natural surface.

Table 1 Conductivity inversion model layer thicknesses and depths.

Layer number	Thickness (m)	Depth to top (m)	Depth to bottom (m)
1	2.00	0.00	2.00
2	2.20	2.00	4.20
3	2.42	4.20	6.62
4	2.66	6.62	9.28
5	2.93	9.28	12.21
6	3.22	12.21	15.43
7	3.54	15.43	18.97
8	3.90	18.97	22.87
9	4.29	22.87	27.16
10	4.72	27.16	31.87
11	5.19	31.87	37.06
12	5.71	37.06	42.77
13	6.28	42.77	49.05
14	6.90	49.05	55.95
15	7.59	55.95	63.54
16	8.35	63.54	71.90
17	9.19	71.90	81.09
18	10.11	81.09	91.20
19	11.12	91.20	102.32
20	12.23	102.32	114.55
21	13.45	114.55	128.00
22	14.80	128.00	142.81
23	16.28	142.81	159.09
24	17.91	159.09	176.99
25	∞	176.99	∞

Data formats:

The data are available in the following formats:

- ER-Mapper (sub-folder: aem\grids\layers\er_mapper). The grids are stored in ER Mapper binary floating point raster grid format (IEEE 4 byte reals) with an associated header (.ers) file. These are the original data supplied by GA.
- ESRI grid (sub-folder: aem\grids\layers\ESRI_grid). The data are stored as ESRI floating point grids, converted from the ER-Mapper grids by ABARES.

3.3 Depth slice grids (sub-folder: aem\grids\depth_slices)

The depth slice grids represent the average conductivity in S/m of various regular intervals (Table 2). They have been derived from the layer conductivity grids by a weighted average of the layers that intersect the depth interval. For example a slice between 5m and 10m depth would be constructed as follows:

$$\frac{(6.62-5)\times layer\ 3\ conductivity + (2.66)\times layer\ 4\ conductivity + (10-9.28)\times layer\ 5\ conductivity}{10-5}$$

Table 2 Depth slice intervals.

Depth to top (m)	Depth to bottom (m)	Thickness (m)
0	5	5
5	10	5
10	15	5
15	20	5
20	30	10
30	40	10
40	60	20
60	80	20
80	100	20
100	150	50
150	200	50

Data formats:
The data are available in the following formats:

- ER-Mapper (sub-folder: aem\grids\depth_slices\er_mapper). The grids are stored in ER Mapper binary floating point raster grid format (IEEE 4 byte reals) with an associated header (.ers) file. These are the original data supplied by GA.
- ESRI grid (sub-folder: aem\grids\depth_slices\ESRI_grid). The data are stored as ESRI floating point grids, converted from the ER-Mapper grids by ABARES.
- Enhanced images (sub-folder: aem\images) as georeferenced JPEG image files (.jpg) with associated world files (.jgw). The image includes an embedded scale bar that shows how the colours correspond to the grid data values. The images were produced from the ER-Mapper grids by GA. Section 3.1 of Fisher and Brodie (2008) gives an overview of the image enhancement techniques used to generate the enhanced images. Two colour stretches are provided:
    - 0-0.5 S/m (equivalent to 0-500 mS/m) pseudocolour histogram equalised colour stretch with an E-W gradient (sub-folder: aem\images\depthslices_he).
    - 0-0.5 S/m (equivalent to 0-500 mS/m) using a pseudocolour linear colour stretch with an E-W gradient (sub-folder: aem\images\depthslices_liner).

3.4 Vertical conductivity sections (sub-folder: aem\sections)

Enhanced images of vertical conductivity depth sections along the line of best fit passing through the flight line were produced from the GA LEI results.

The sections were outputted as coloured images in JPEG and PDF formats, with a horizontal scale of 1:100 000 and a vertical scale of 1:5 000 (vertical exaggeration of 20). These scales are only relevant when viewing the products at their original page/image size. A colour scale is included, as is the location (eastings and northings) of each flight line.

Two sets of sections were produced:

- a pseudocolour linear colour stretch using a data range of 0-0.5 S/m (sub-folder: aem\sections\linear_0.0_0.5).
- a pseudocolour logarithmic colour stretch using a data range of 0.01-1 S/m (sub-folder: aem\sections\log_0.01_1.00).

3.5 Conductance distribution (sub-folder: aem\grids\conductance).

A grid and images of conductance distribution produced from the GA LEI results. Conductance is conductivity multiplied by thickness, and is measured in siemens (S).

Data formats:
The data are available in the following formats:

- ER-Mapper (sub-folder: aem\grids\conductance\er_mapper). The grids are stored in ER Mapper binary floating point raster grid format (IEEE 4 byte reals) with an associated header (.ers) file. These are the original data supplied by GA.
- ESRI grid (sub-folder: aem\grids\conductance\ESRI_grid). The data are stored as ESRI floating point grids, converted from the ER-Mapper grids by ABARES.
- Enhanced images (sub-folder: aem\images\conductance) as georeferenced JPEG image files (.jpg) with associated world files (.jgw). The image includes an embedded scale bar that shows how the colours correspond to the grid data values. The images were produced from the ER-Mapper grids by GA. Section 3.1 of Fisher and Brodie (2008) gives an overview of the image enhancement techniques used to generate the enhanced images. Two images were produced:
    - 0 to 30 S pseudocolour linear colour stretch with an E-W gradient.
    - 0 to 30 S pseudocolour histogram equalised colour stretch with an E-W gradient.

3.6 Base of the conductive unit (sub-folder: aem\grids\conductivity_base).

An automated technique was applied to the point located GA LEI to create products based on the depth of the base of the conductive unit. Two sets of grids and images were produced:

- elevation of the base of the conductive unit
- depth of the base of the conductive unit below the ground surface.

Data formats:
The data are available in the following formats:

- ER-Mapper (sub-folder: aem\grids\conductivity_base\er_mapper). The grids are stored in ER Mapper binary floating point raster grid format (IEEE 4 byte reals) with an associated header (.ers) file. These are the original data supplied by GA.
- ESRI grid (sub-folder: aem\grids\conductivity_base\ESRI_grid). The data are stored as ESRI floating point grids, converted from the ER-Mapper grids by ABARES.
- Enhanced images (sub-folder: aem\images\conductivity_base) as georeferenced JPEG image files (.jpg) with associated world files (.jgw). The image includes an embedded scale bar that shows how the colours correspond to the grid data values. The images were produced from the ER-Mapper grids by GA. Section 3.1 of Fisher and Brodie (2008) gives an overview of the image enhancement techniques used to generate the enhanced images. Two images were produced:
    - a rainbow1 linear colour stretch with an E-W gradient of the depth of the conductive layer.
    - a rainbow1 linear colour stretch with an E-W gradient of elevation of the conductive layer.

3.7 Enhanced images of AEM datasets (sub-folder: aem\images)

A range of images of the GA-LEI AEM grid datasets were produced using standard image enhancement techniques, and have been described in the relevant sections above.

4.0 MAGSPEC data

The MAGSPEC survey was acquired by Kevron between the 23rd of May and the 12th of July 2001. The aircraft was fitted with a horizontal gradiometer system to measure magnetic anomalies, and a downward looking gamma-ray spectrometer that measured the naturally occurring gamma rays emanating from radioactive materials at the earth's surface. Ground elevation was also determined from the survey data, by subtracting radar altimeter measurements of the aircraft's height above the ground, from GPS measurement of its height above sea level.

This data package includes the gridded MAGSPEC data products (magnetic, gamma-ray and elevation data) for the 'Billabong Creek, NSW, MAGSPEC survey (GA Project # 908)', released previously through the Geoscience Australia 'Geophysical Archive Data Delivery System' (GADDS), (www.geoscience.gov.au/gadds), together with the addition of the enhanced products and images described below. The final point located data for the Billabong Creek MAGSPEC survey are available via GADDS, and are not included in this dataset.

The MAGSPEC datasets are:

- airborne magnetic data comprising grids of total magnetic intensity (TMI), TMI reduced to pole (TMI-RTP) and TMI-RTP first vertical derivative data. A range of enhanced magnetic images were derived from the data
- airborne gamma-ray data comprising grids of dose rate, concentration of potassium (K), thorium (Th) and uranium (U). A range of enhanced gamma-ray images were derived from the data
- elevation data comprising grids and images of the digital elevation model (DEM) derived from the MAGSPEC survey.

4.1 Magnetics data (sub-folder: magspec\grids\mag)

Section 2.2 of Fisher and Brodie (2008) (Geophysical survey data and metadata report) describes the acquisition and processing of the Billabong Creek MAGSPEC survey magnetic data.

Section 3.3 of Fisher and Brodie (2008) describes the methods used to create enhanced images that were derived from these grids, namely, total magnetic intensity (TMI), TMI reduced to pole (TMI-RTP) and TMI-RTP first vertical derivative data. Section 3.1 of Fisher and Brodie (2008) gives an overview of the image enhancement techniques used to generate the enhanced images.

Data formats:
The data are available in the following formats:

- ER-Mapper (sub-folder: magspec\grids\mag\er_mapper). The grids are stored in ER Mapper binary floating point raster grid format (IEEE 4 byte reals) with an associated header (.ers) file. These are the original data supplied by GA.
- ESRI grid (sub-folder: magspec\grids\mag\er_mapper\ESRI_grid). The data are stored as ESRI floating point grids, converted from the ER-Mapper grids by ABARES.

- Enhanced images (sub-folder: magspec\images\mag) as georeferenced JPEG image files (.jpg) with associated world files (.jgw). The images include an embedded scale bar that shows how the colours correspond to the values of grid data. The images were produced from the ER-Mapper grids by GA.

Appendix 1 gives a detailed list of the contents of each directory.

4.2 Gamma-ray data (sub-folder: magspec\grids\rad)

Section 2.2 of Fisher and Brodie (2008) (Geophysical survey data and metadata report) describes the acquisition and processing of the Billabong Creek MAGSPEC survey gamma-ray data.

Section 3.4 of Fisher and Brodie (2008) describes the methods used to create enhanced images that were derived from the airborne gamma-ray data grids, namely: K-Th-U ternary image, dose rate, concentration of potassium (K), thorium (Th) and uranium (U). Section 3.1 of Fisher and Brodie (2008) gives an overview of the image enhancement techniques used to generate the enhanced images.

Data formats:
The data are available in the following formats:

- ER-Mapper (sub-folder: magspec\grids\rad\er_mapper). The grids are stored in ER Mapper binary floating point raster grid format (IEEE 4 byte reals) with an associated header (.ers) file. These are the original data supplied by GA.
- ESRI grid (sub-folder: magspec\grids\rad\er_mapper\ESRI_grid). The data are stored as ESRI floating point grids, converted from the ER-Mapper grids by ABARES.
- Enhanced images (sub-folder: magspec\images\rad) as georeferenced JPEG image files (.jpg) with associated world files (.jgw). The images include an embedded scale bar that shows how the colours correspond to the values of grid data. The images were produced from the ER-Mapper grids by GA.

Appendix 1 gives a detailed list of the contents of each directory.

4.3 Digital Elevation Model (DEM) data (sub-folder: magspec\grids\dem)

Section 2.2 of Fisher and Brodie (2008) (Geophysical survey data and metadata report) describes the acquisition and processing of the Billabong Creek MAGSPEC survey elevation data.

Section 3.5 of Fisher and Brodie (2008) describes the methods used to create enhanced images that were derived from these grids, namely, a DEM enhanced image. Section 3.1 of Fisher and Brodie (2008) gives an overview of the image enhancement techniques used to generate the enhanced images.

Data formats:
The data are available in the following formats:

- ER-Mapper (sub-folder: magspec\grids\dem\er_mapper). The grids are stored in ER Mapper binary floating point raster grid format (IEEE 4 byte reals) with an associated header (.ers) file. These are the original data supplied by GA.
- ESRI grid (sub-folder: magspec\grids\dem\ESRI_grid). The data are stored as ESRI floating point grids, converted from the ER-Mapper grids by ABARES.

- Enhanced images (sub-folder: magspec\images\dem) as georeferenced JPEG image files (.jpg) with associated world files (.jgw). The image includes an embedded scale bar that shows how the colours correspond to the values of elevation (m). The images were produced from the ER-Mapper grids by GA.

Appendix 1 gives a detailed list of the contents of each directory.

5.0 Gravity data (sub-folder: gravity\grids)

Section 2.3 of Fisher and Brodie (2008) (Geophysical survey data and metadata report) describes the acquisition and processing of the Australian National Gravity Database for the Billabong Creek area.

Section 3.6 of Fisher and Brodie (2008) describes the methods used to create enhanced images that were derived from these grids, namely, an enhanced gravity image. Section 3.1 of Fisher and Brodie (2008) gives an overview of the image enhancement techniques used to generate the enhanced images.

Data formats:
The data are available in the following formats:

- ER-Mapper (sub-folder: gravity\grids\er_mapper). The grids are stored in ER Mapper binary floating point raster grid format (IEEE 4 byte reals) with an associated header (.ers) file. These are the original data supplied by GA.
- ESRI grid (sub-folder: gravity\grids\ESRI_grid). The data are stored as ESRI floating point grids, converted from the ER-Mapper grids by ABARES.
- Enhanced images (sub-folder: gravity\images) as georeferenced JPEG image files (.jpg) with associated world files (.jgw). The images include an embedded scale bar that shows how the colours correspond to the values of grid data. The images were produced from the ER-Mapper grids by GA.
- Point data (sub-folder: gravity\point_data) of gravity survey station data
- An ESRI shapefile (sub-folder: gravity\shapefiles) of the location of the gravity survey stations used to create the gridded gravity data was produced (point data).

Appendix 1 gives a detailed list of the contents of each directory.

Appendix 1. Details of the accompanying data package

Directory	File name	File description
aem\grids\conductance\er-mapper	conductance_000m_200m.ers	40 m grid of conductance between 0-200 m depth derived from the GA LEI
aem\grids\conductance\esri_grid	condc_000_200	40 m grid of conductance between 0-200 m depth derived from the GA LEI
aem\grids\conductivity_base\er-mapper	conductivity_base_depth.ers	40 m grid of the depth of the base of the conductive layer derived from the GA LEI
	conductivity_base_elevation.ers	40 m grid of elevation of the base of the conductive layer derived from the GA LEI
aem\grids\conductivity_base\esri_grid	con_base_dpth	40 m grid of the depth of the base of the conductive layer derived from the GA LEI
	con_base_elev	40 m grid of elevation of the base of the conductive layer derived from the GA LEI
aem\grids\depthslices\er-mapper	depthslice_000_005.ers	40 m grid of conductivity in the 0-5 m depth slice produced by the GA-LEI
	depthslice_005_010.ers	40 m grid of conductivity in the 5-10 m depth slice produced by the GA-LEI
	depthslice _010_015.ers	40 m grid of conductivity in the 10-15 m depth slice produced by the GA-LEI
	depthslice _015_020.ers	40 m grid of conductivity in the 15-20 m depth slice produced by the GA-LEI
	depthslice _020_030.ers	40 m grid of conductivity in the 20-30 m depth slice produced by the GA-LEI
	depthslice _030_040.ers	40 m grid of conductivity in the 30-40 m depth slice produced by the GA-LEI
	depthslice _040_060.ers	40 m grid of conductivity in the 40-60 m depth slice produced by the GA-LEI
	depthslice _060_080.ers	40 m grid of conductivity in the 60-80 m depth slice produced by the GA-LEI
	depthslice _080_100.ers	40 m grid of conductivity in the 80-100 m depth slice produced by the GA-LEI
	depthslice _100_150.ers	40 m grid of conductivity in the 100-150 m depth slice produced by the GA-LEI
	depthslice _150_200.ers	40 m grid of conductivity in the 150-200 m depth slice produced by the GA-LEI
aem\grids\depthslices\esri_grid	ds_000_005	40 m grid of conductivity in the 0-5 m depth slice produced by the GA-LEI
	ds_005_010	40 m grid of conductivity in the 5-10 m depth slice produced by the GA-LEI
	ds_010_015	40 m grid of conductivity in the 10-15 m depth slice produced by the GA-LEI
	ds_015_020	40 m grid of conductivity in the 15-20 m depth slice produced by the GA-LEI
	ds_020_030	40 m grid of conductivity in the 20-30 m depth slice produced by the GA-LEI
	ds_030_040	40 m grid of conductivity in the 30-40 m depth slice produced by the GA-LEI
	ds_040_060	40 m grid of conductivity in the 40-60 m depth slice produced by the GA-LEI
	ds_060_080	40 m grid of conductivity in the 60-80 m depth slice produced by the GA-LEI
	ds_080_100	40 m grid of conductivity in the 80-100 m depth slice produced by the GA-LEI
	ds_100_150	40 m grid of conductivity in the 100-150 m depth slice produced by the GA-LEI
	ds_150_200	40 m grid of conductivity in the 150-200 m depth slice produced by the GA-LEI
aem\grids\layers\er-mapper	layer_01.ers	40 m grid of conductivity for layer 1 (0.00-2.00 m) produced by the GA-LEI
	layer_02.ers	40 m grid of conductivity for layer 2 (2.00-4.20 m) produced by the GA-LEI
	layer_03.ers	40 m grid of conductivity for layer 3 (4.20-6.62 m) produced by the GA-LEI
	layer_04.ers	40 m grid of conductivity for layer 4 (6.62-9.28 m) produced by the GA-LEI
	layer_05.ers	40 m grid of conductivity for layer 5 (9.28-12.21 m) produced by the GA-LEI
	layer_06.ers	40 m grid of conductivity for layer 6 (12.21-15.43 m) produced by the GA-LEI
	layer_07.ers	40 m grid of conductivity for layer 7 (15.43-18.97 m) produced by the GA-LEI
	layer_08.ers	40 m grid of conductivity for layer 8 (18.97-22.87 m) produced by the GA-LEI
	layer_09.ers	40 m grid of conductivity for layer 9 (22.87-27.16 m) produced by the GA-LEI
	layer_10.ers	40 m grid of conductivity for layer 10 (27.16-31.87 m) produced by the GA-LEI

Directory	File name	File description
	layer_11.ers	40 m grid of conductivity for layer 11 (31.87-37.06 m) produced by the GA-LEI
	layer_12.ers	40 m grid of conductivity for layer 12 (37.06-42.77 m) produced by the GA-LEI
	layer_13.ers	40 m grid of conductivity for layer 13 (42.77-49.04 m) produced by the GA-LEI
	layer_14.ers	40 m grid of conductivity for layer 14 (49.04-55.95 m) produced by the GA-LEI
	layer_15.ers	40 m grid of conductivity for layer 15 (55.95-63.54 m) produced by the GA-LEI
	layer_16.ers	40 m grid of conductivity for layer 16 (63.54-71.90 m) produced by the GA-LEI
	layer_17.ers	40 m grid of conductivity for layer 17 (71.90-81.09 m) produced by the GA-LEI
	layer_18.ers	40 m grid of conductivity for layer 18 (81.09-91.20 m) produced by the GA-LEI
	layer_19.ers	40 m grid of conductivity for layer 19 (91.20-102.32 m) produced by the GA-LEI
	layer_20.ers	40 m grid of conductivity for layer 20 (102.32-114.55 m) produced by the GA-LEI
	layer_21.ers	40 m grid of conductivity for layer 21 (114.55-128.00 m) produced by the GA-LEI
	layer_22.ers	40 m grid of conductivity for layer 22 (128.00-142.80 m) produced by the GA-LEI
	layer_23.ers	40 m grid of conductivity for layer 23 (142.80-159.09 m) produced by the GA-LEI
	layer_24.ers	40 m grid of conductivity for layer 24 (159.09-176.99 m) produced by the GA-LEI
	layer_25.ers	40 m grid of conductivity for layer 25 (176.99-∞ m) produced by the GA-LEI
aem\grids\layers\esri_grid	layer_01	40 m grid of conductivity for layer 1 (0.00-2.00 m) produced by the GA-LEI
	layer_02	40 m grid of conductivity for layer 2 (2.00-4.20 m) produced by the GA-LEI
	layer_03	40 m grid of conductivity for layer 3 (4.20-6.62 m) produced by the GA-LEI
	layer_04	40 m grid of conductivity for layer 4 (6.62-9.28 m) produced by the GA-LEI
	layer_05	40 m grid of conductivity for layer 5 (9.28-12.21 m) produced by the GA-LEI
	layer_06	40 m grid of conductivity for layer 6 (12.21-15.43 m) produced by the GA-LEI
	layer_07	40 m grid of conductivity for layer 7 (15.43-18.97 m) produced by the GA-LEI
	layer_08	40 m grid of conductivity for layer 8 (18.97-22.87 m) produced by the GA-LEI
	layer_09	40 m grid of conductivity for layer 9 (22.87-27.16 m) produced by the GA-LEI
	layer_10	40 m grid of conductivity for layer 10 (27.16-31.87 m) produced by the GA-LEI
	layer_11	40 m grid of conductivity for layer 11 (31.87-37.06 m) produced by the GA-LEI
	layer_12	40 m grid of conductivity for layer 12 (37.06-42.77 m) produced by the GA-LEI
	layer_13	40 m grid of conductivity for layer 13 (42.77-49.04 m) produced by the GA-LEI
	layer_14	40 m grid of conductivity for layer 14 (49.04-55.95 m) produced by the GA-LEI
	layer_15	40 m grid of conductivity for layer 15 (55.95-63.54 m) produced by the GA-LEI
	layer_16	40 m grid of conductivity for layer 16 (63.54-71.90 m) produced by the GA-LEI
	layer_17	40 m grid of conductivity for layer 17 (71.90-81.09 m) produced by the GA-LEI
	layer_18	40 m grid of conductivity for layer 18 (81.09-91.20 m) produced by the GA-LEI
	layer_19	40 m grid of conductivity for layer 19 (91.20-102.32 m) produced by the GA-LEI
	layer_20	40 m grid of conductivity for layer 20 (102.32-114.55 m) produced by the GA-LEI
	layer_21	40 m grid of conductivity for layer 21 (114.55-128.00 m) produced by the GA-LEI
	layer_22	40 m grid of conductivity for layer 22 (128.00-142.80 m) produced by the GA-LEI
	layer_23	40 m grid of conductivity for layer 23 (142.80-159.09 m) produced by the GA-LEI
	layer_24	40 m grid of conductivity for layer 24 (159.09-176.99 m) produced by the GA-LEI
	layer_25	40 m grid of conductivity for layer 25 (176.99-∞ m) produced by the GA-LEI
aem\images\conductance	conductance_000m_200m_he.jpg	pseudocolour linear stretch with a E-W gradient of the conductance grid
	conductance_000m_200m_linear.jpg	pseudocolour histogram equalised with a E-W gradient of the conductance grid

Directory	File name	File description
aem\images\conductivity_base	conductivity_base_depth_linear.jpg	rainbow1 linear stretch with a E-W gradient of interpreted basement depth
	conductivity_base_elevation_linear.jpg	rainbow1 linear stretch with a E-W gradient of interpreted basement elevation
aem\images\depthslices_he	depthslice_000m_005m_he.jpg	pseudocolour histogram equalised with a E-W gradient of the conductivity depth slice
	depthslice_005m_010m_he.jpg	pseudocolour histogram equalised with a E-W gradient of the conductivity depth slice
	depthslice_010m_015m_he.jpg	pseudocolour histogram equalised with a E-W gradient of the conductivity depth slice
	depthslice_015m_020m_he.jpg	pseudocolour histogram equalised with a E-W gradient of the conductivity depth slice
	depthslice_020m_030m_he.jpg	pseudocolour histogram equalised with a E-W gradient of the conductivity depth slice
	depthslice_030m_040m_he.jpg	pseudocolour histogram equalised with a E-W gradient of the conductivity depth slice
	depthslice_040m_060m_he.jpg	pseudocolour histogram equalised with a E-W gradient of the conductivity depth slice
	depthslice_060m_080m_he.jpg	pseudocolour histogram equalised with a E-W gradient of the conductivity depth slice
	depthslice_080m_100m_he.jpg	pseudocolour histogram equalised with a E-W gradient of the conductivity depth slice
aem\images\depthslices_linear	depthslice_000m_005m_linear.jpg	pseudocolour linear stretch with a E-W gradient of the conductivity depth slice
	depthslice_005m_010m_linear.jpg	pseudocolour linear stretch with a E-W gradient of the conductivity depth slice
	depthslice_010m_015m_linear.jpg	pseudocolour linear stretch with a E-W gradient of the conductivity depth slice
	depthslice_015m_020m_linear.jpg	pseudocolour linear stretch with a E-W gradient of the conductivity depth slice
	depthslice_020m_030m_linear.jpg	pseudocolour linear stretch with a E-W gradient of the conductivity depth slice
	depthslice_030m_040m_linear.jpg	pseudocolour linear stretch with a E-W gradient of the conductivity depth slice
	depthslice_040m_060m_linear.jpg	pseudocolour linear stretch with a E-W gradient of the conductivity depth slice
	depthslice_060m_080m_linear.jpg	pseudocolour linear stretch with a E-W gradient of the conductivity depth slice
	depthslice_080m_100m_linear.jpg	pseudocolour linear stretch with a E-W gradient of the conductivity depth slice
	depthslice_100m_150m_linear.jpg	pseudocolour linear stretch with a E-W gradient of the conductivity depth slice
	depthslice_150m_200m_linear.jpg	pseudocolour linear stretch with a E-W gradient of the conductivity depth slice
aem\line_data	billabong_creek_inversion.dat	final point located AEM data produced by the GA-LEI (see .hdr file for details)
	billabong_creek_tempest.dat	final point located data from the AEM survey (see .hdr file for details)
aem\sections\linear_0.0_0.5\jpg	*.jpg	pseudocolour linear stretch conductivity-depth section of the 181 flightlines
aem\sections\linear_0.0_0.5\pdf	*.pdf	as above, in pdf format
aem\sections\log_0.01_1.00\jpg	*.jpg	pseudocolour logarithmic stretch conductivity-depth section of the 181 flightlines
aem\sections\log_0.01_1.00\pdf	*.pdf	as above, in pdf format
gravity\grids\er-mapper	billabong_grav_2km.ers	2 km grid of gravity data
gravity\grids\esri_grid	bbong_grav2km	2 km grid of gravity data
gravity\images	regional_grav_enhanced.jpg	pseudocolour histogram equalised image of regional gravity data with a NE gradient
	grav_enhanced.jpg	pseudocolour histogram equalised image of gravity data with a NE gradient
gravity\point_data	billabong_grav.dat	point located gravity survey station data (see readme.txt for details)
gravity\shapefiles	billabong_grav_stations.shp	locations of gravity survey stations
magspec\grids\dem\er-mapper	billabong_dem_magspec.ers	20m grid of elevation, derived from MAGSPEC survey
magspec\grids\dem\esri_grid	dem_magspec	20m grid of elevation, derived from MAGSPEC survey
magspec\grids\mag\er-mapper	billabong_tmi.ers	20 m grid of total magnetic intensity (TMI)
	billabong_tmirtp.ers	20 m grid of TMI reduced to the pole (RTP)
	billabong_tmirtpvd1.ers	20 m grid of the 1st vertical derivative (VD1) of the TMI RTP
magspec\grids\mag\esri_grid	bb_tmi	20 m grid of total magnetic intensity (TMI)

Directory	File name	File description
	bb_tmirtp	20 m grid of TMI reduced to the pole (RTP)
	bb_tmirtpvd1	20 m grid of the 1st vertical derivative (VD1) of the TMI RTP
magspec\grids\rad\er-mapper	billabong_dose.ers	20 m grid of dose rate data (nG.hr^{-1}), derived from total count channel
	billabong_potassium.ers	20 m grid of equivalent concentration of potassium (percent)
	billabong_thorium.ers	20 m grid of equivalent concentration of thorium (eppm)
	billabong_uranium.ers	20 m grid of equivalent concentration of uranium (eppm)
magspec\grids\rad\esri_grid	bb_dose	20 m grid of dose rate data (nG.hr^{-1}), derived from total count channel
	bb_potassium	20 m grid of equivalent concentration of potassium (percent)
	bb_thorium	20 m grid of equivalent concentration of thorium (eppm)
	bb_uranium	20 m grid of equivalent concentration of uranium (eppm)
magspec\images\dem	dem_magspec_enhanced.jpg	rainbow1 histogram equalised image of elevation with a NE gradient
magspec\images\mag	tmi_hsi_enhanced.jpg	rain_gomp histogram equalised image of TMI with a NE gradient
	tmi_raingomp.jpg	rain-gomp histogram equalised image of TMI
	tmirtp_hsi_enhanced.jpg	rain_gomp histogram equalised image of TMI RTP with a NE gradient
	tmirtp_raingomp.jpg	rain-gomp histogram equalised image of TMI RTP
	tmirtpvd1_grey.jpg	greyscale histogram equalised image of TMI RTP VD1
	tmirtpvd1_raingomp.jpg	rain-gomp histogram equalised image of TMI RTP VD1
magspec\images\rad	dose_enhanced.jpg	rain-gomp histogram equalised image of the dose rate with a NE gradient
	k_enhanced.jpg	rain-gomp histogram equalised image of equivalent concentration of potassium with a NE gradient
	kthu_ternary.jpg	histogram equalised image with potassium-red, thorium-green and uranium-blue
	th_enhanced.jpg	rain-gomp histogram equalised image of equivalent concentration of thorium with a NE gradient
	u_enhanced.jpg	rain-gomp histogram equalised image of equivalent concentration of uranium count with a NE gradient
reports	BBC_Fugro_AEM_jobreport.pdf	PDF file of the Fugro Airborne Services (FAS) acquisition and processing report. This report summarises the procedures and equipment used by FAS in the acquisition, verification and processing of the airborne geophysical data.
	BBC_Inversion_Report_final.pdf	PDF file of AEM Inversion report from Geoscience Australia. This report describes the geophysical inversion of the Billabong Creek TEMPEST airborne electromagnetic (AEM) survey data to produce subsurface electrical conductivity predictions using a layered earth inversion algorithm developed by Geoscience Australia (GA-LEI).
	BBC_survey_and_metadata_final.pdf	PDF file of Geophysical survey data and metadata report from Geoscience Australia. This report describes the data sets that have been acquired and processed, and the products that have been derived from those datasets.
	HSK_KEVRON_Operations_Processing_Report.pdf	PDF file of the Kevron Geophysics report for the Bureau of Rural Sciences. It describes the operations and processing of data from the Honeysuckle Creek and Billabong Creek airborne geophysical surveys that Kevron Geophysics flew between May and July 2001.

Notes:

- All grids (ER-Mapper and ESRI Grids), images (.jpg) and shapefiles (.shp) are located in the Geodetic Datum of Australia, Map Grid of Australia Zone 55 coordinate system.

- The jpg images can be viewed in many software packages, and they also have associated world files (.jgw) and projection files (.xml) that contain spatial reference information for viewing in GIS software, such as ESRI ArcGIS.

- To view ER-Mapper grids (.ers format) and ER-Mapper algorithm images (.alg), you will need to download the ER Mapper Plugin appropriate to your GIS system. These are available for free download from: http://www.erdas.com

- The above GIS data have been tested using ESRI ArcGIS ArcMap version 9.2, with the ER Mapper plugin "ArcGIS 8.x and 9.x ECW JPEG 2000 plugin" version 4.2.